Quality difference of neointima following the implantation of everolimus-eluting bioresorbable scaffolds and metallic stents in patients with ST-elevation myocardial infarction: quantitative assessments by light intensity, light attenuation, and backscatter on optical coherence tomography in the TROFI II trial

Yohei Sotomi[1], MD, PhD; Yoshinobu Onuma[2,3], MD, PhD; Shengnan Liu[4], Msc; Taku Asano[1], MD; Jeroen Eggermont[4], PhD; Yuki Katagiri[1], MD; Rafael Cavalcante[2], MD, PhD; Robbert J. de Winter[1], MD, PhD; Joanna J. Wykrzykowska[1], MD, PhD; Salvatore Brugaletta[5], MD, PhD; Lorenz Räber[6], MD, PhD; Manel Sabaté[5], MD, PhD; Stephan Windecker[6], MD; Jouke Dijkstra[4], PhD; Patrick W. Serruys[7]*, MD, PhD

1. Academic Medical Center, University of Amsterdam, Amsterdam, the Netherlands; 2. Thoraxcenter, Erasmus Medical Center, Rotterdam, the Netherlands; 3. Cardialysis, Rotterdam, the Netherlands; 4. LKEB–Division of Image Processing, Department of Radiology, Leiden University Medical Center, Leiden, the Netherlands; 5. Hospital Clinic, Institut Clinic Cardiovascular, Institut d'Investigacions Biomèdiques August Pi i Sunyer (IDIBAPS), University of Barcelona, Barcelona, Spain; 6. Bern University Hospital, Bern, Switzerland; 7. International Centre for Circulatory Health, NHLI, Imperial College London, London, United Kingdom

GUEST EDITOR: Alec Vahanian, MD, PhD; *Department of Cardiology, Hôpital Bichat, Paris and University Paris VII, Paris, France*

This paper also includes supplementary data published online at: http://www.pcronline.com/eurointervention/139th_issue/117

Abstract

Aims: We aimed to assess possible differences in neointimal quality after everolimus-eluting bioresorbable scaffold (BVS) implantation in comparison with cobalt-chromium everolimus-eluting scaffold (CoCr-EES) implantation by optical frequency domain imaging (OFDI).

Methods and results: This study is a *post hoc* analysis of the TROFI II trial assessing neointimal quality six months after the implantation of BVS (N=82) and CoCr-EES (N=87) in STEMI patients. Neointimal light property analysis by OFDI fully automatically computed light attenuation, backscatter and light intensity for superficial and deep neointima. High light attenuation/backscatter and high light intensity are reportedly associated with lipidic change and tissue maturation, respectively. Superficial and deep neointima in BVS presented lower light attenuation than CoCr-EES (superficial: 0.77 ± 0.15 vs. 1.27 ± 0.55 mm^{-1}, p<0.001; deep: 0.88 ± 0.20 vs. 1.17 ± 0.27 mm^{-1}, p<0.001). Superficial neointima in BVS showed comparable backscatter to that of CoCr-EES (4.81 ± 0.52 vs. 4.94 ± 0.61, p=0.141), while deep neointima in BVS showed lower backscatter than that of CoCr-EES (4.60 ± 0.62 vs. 4.97 ± 0.62, p<0.001). Light intensity of superficial neointima was comparable between both arms (139 ± 13 vs. 144 ± 30, p=0.236), whereas light intensity of deep neointima in BVS was lower than CoCr-EES (129 ± 14 vs. 138 ± 21, p<0.001).

Conclusions: The present OFDI comparison suggested that tissue maturation was comparable but lipidic change of neointima was less prominent after BVS than after CoCr-EES implantation. ClinicalTrials.gov Identifier: NCT01986803

*Corresponding author: Cardiovascular Science Division of the NHLI within Imperial College of Science, Technology and Medicine, South Kensington Campus, London, SW7 2AZ, United Kingdom. E-mail: patrick.w.j.c.serruys@gmail.com

Abbreviations

BVS   bioresorbable vascular scaffold
CoCr-EES cobalt-chromium everolimus-eluting scaffold
OCT   optical coherence tomography
OFDI   optical frequency domain imaging
PCI   percutaneous coronary intervention
PSLIA   peri-strut low-intensity area
STEMI   ST-elevation myocardial infarction

Introduction

Recent reports from randomised trials and registry data evaluating the everolimus-eluting Absorb™ bioresorbable vascular scaffold (Absorb BVS; Abbott Vascular, Santa Clara, CA, USA) have revealed a relatively high incidence of early and late scaffold thrombosis[1,2]. Physicians continue to make every effort to understand the pathophysiological cause of scaffold thrombosis. Optical coherence tomography (OCT) assessments of scaffold thrombosis cases have demonstrated that a peri-strut low-intensity area (PSLIA) is one of the major imaging findings associated with scaffold thrombosis[3]. PSLIA is defined as homogenously appearing, non-signal-attenuating zones around struts of lower intensity than the surrounding tissue, which might be correlated with vascular oedema and vulnerability[4]. Although the direct relationship between this finding and scaffold thrombosis still remains unknown, the quality assessment of neointimal growth would be a key to obtaining a better understanding of the underlying pathogenic mechanism of scaffold thrombosis.

Several studies have reported the usefulness of OCT light intensity, light attenuation and light backscatter to characterise the tissue components of the coronary artery. In a histological study, it was demonstrated that increased light attenuation and light backscatter were associated with lipid-rich plaque and macrophages[5,6]. Van Soest et al reported that necrotic core and macrophage infiltration exhibit strong attenuation, while calcific and fibrous tissue have a lower light attenuation[7]. Nakano et al evaluated 14 human stented coronaries with optical frequency domain imaging (OFDI) and demonstrated that light attenuation and light intensity were associated with morphological features of in-stent neointima[8]. Malle et al reported the correlation of greyscale signal intensity (light intensity) and maturation of the neointimal tissue[9]. Nakatani et al demonstrated the association of light intensity with the biointegration process of BVS in porcine models[10]. This supports the use of OCT light property analysis for the quantitative assessment of the tissue components.

It could be hypothesised that the quality of neointima after the implantation of BVS would be dissimilar to that of metallic stents and that the differential neointima could lead to differential clinical outcomes. In the present study, we evaluated the neointimal light intensity, light attenuation, and light backscatter on OCT as a surrogate of neointimal quality six months after the implantation of BVS in comparison with cobalt-chromium everolimus-eluting scaffolds (CoCr-EES) using dedicated software in patients with ST-elevation myocardial infarction (STEMI) from the TROFI II randomised controlled trial[11].

Methods

STUDY DESIGN AND POPULATION

The present study is a *post hoc* substudy of the TROFI II trial focusing on the quantitative neointimal quality assessment after the implantation of BVS and CoCr-EES. The TROFI II trial is a multicentre, international (eight centres in four countries), randomised, two-arm, single-blind, controlled trial performed in STEMI patients (clinicaltrials.gov, NCT01986803). This is an investigator-initiated trial, sponsored by the European Cardiovascular Research Institute (ECRI). The details of the protocol and the main results of the trial have already been reported elsewhere[11]. Briefly, the study included patients presenting with STEMI. All patients were randomised 1:1 to one of the two treatment arms: BVS vs. CoCr-EES (XIENCE Xpedition® stent; Abbott Vascular). All centres had the approval of their medical ethics committee.

PCI PROCEDURE

Details of the percutaneous coronary intervention (PCI) procedure are provided in **Supplementary Appendix 1**[11-13].

OPTICAL FREQUENCY DOMAIN IMAGING ANALYSIS

Angiographic and intracoronary imaging follow-up was conducted six months after the index procedure. OFDI assessment of the stented/scaffolded coronary segment was performed using the Lunawave® console and the FastView® catheter (both Terumo Corp., Tokyo, Japan). The off-line OFDI measurements were performed with QIvus software (Medis, Leiden, the Netherlands) by the core laboratory (Cardialysis B.V., Rotterdam, the Netherlands). With adjustment for the pullback speed, the analysis of continuous cross-sections was performed at each 1 mm longitudinal interval within the treated segment. It was not possible to blind the analysts to the device type based on the characteristic appearance of BVS and CoCr-EES stent struts. Taking into account the difference in optical properties of cobalt-chromium and polylactide, OFDI analysis was performed using comparative methods[14].

In the current *post hoc* study, light property analysis was additionally performed to investigate the neointimal quality quantitatively by independent investigators (Y. Sotomi, T. Asano, Y. Katagiri and R. Cavalcante). Dedicated software was employed for the quantitative light property analysis of the vessel wall (QCU-CMS software version 4.69; Leiden University Medical Center, Leiden, the Netherlands). The software was used to calculate the attenuation and backscattering coefficients based on a depth-resolved (DR) model[15]. The following parameters were analysed within the neointimal area of interest defined with the contours delineated by the core laboratory (Cardialysis): 1) light intensity (no unit), 2) light attenuation (mm^{-1}), and 3) backscatter (no unit).

Figure 1 illustrates the methodology and an example of OCT light property analysis. The light intensity indicates the amount of light signal detected at a certain location in the vessel wall based on reflection and backscatter. The light attenuation, estimated as the DR attenuation coefficient in this study, indicates how fast the light signal is decayed. It is the rate of exponential decreasing intensity
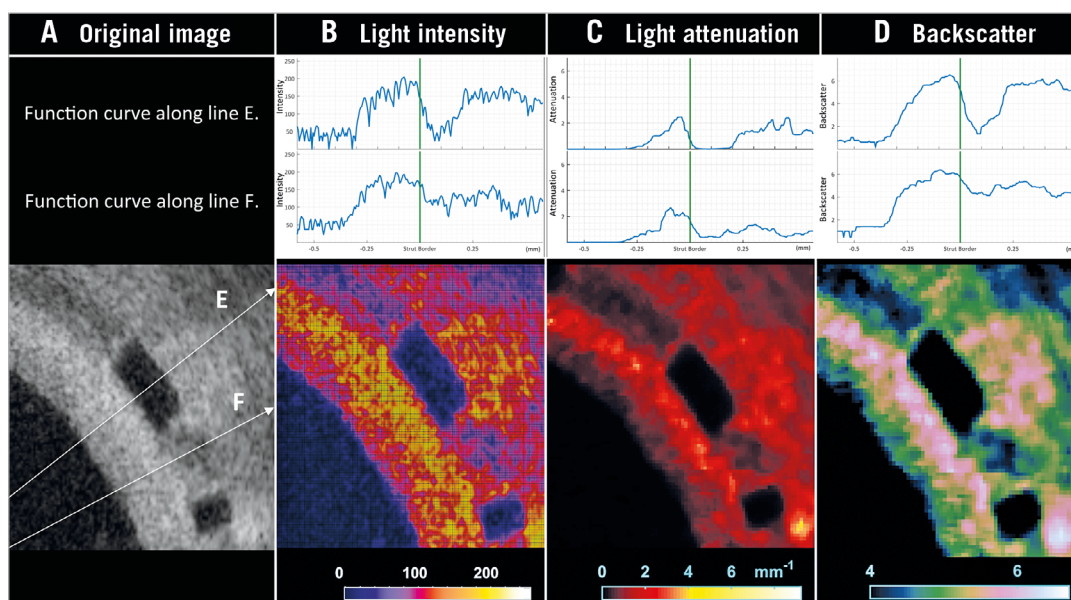
Figure 1. *OCT image example of light intensity, light attenuation, and backscatter analyses. An image example of light property analysis is presented. Based on the original image (A), the dedicated software fully automatically computed three components of light property analysis: 1) light intensity (B), 2) light attenuation (C), and 3) backscatter (D). The upper panels indicate the function curves of each parameter along the lines E and F. The lower panels show the colour-coded images of each parameter.*

related to the light propagation depth. Concretely, the total incident light power I_0 is decreased to be I_0/e at depth $1/\mu_t$. The backscatter, estimated as the DR backscattering coefficient in this study, is related to the efficiency of tissue scattering the light backwards[15].

The neointimal area of interest was assessed separately as the following three parts: 1) superficial neointima (delineated by the luminal contour and the interpolated contour connecting the endoluminal edges of struts [endoluminal stent/scaffold contour]), 2) deep neointima (delineated by the endoluminal and abluminal stent/scaffold contours, excluding strut area), and 3) entire (superficial AND deep) neointima **(Figure 2)**. Each parameter was computed at every cross-section as an average and standard deviation (SD) in the area of interest. The mean value in each scaffold/stent lesion was calculated at lesion level. The reproducibility of the neointimal analysis depends only on the contour delineation since the software is fully automatic. In the current study, the contour delineation was performed by the core lab, and its reproducibility was reported elsewhere[14].

STATISTICAL ANALYSIS
Details of the statistical analysis are described in **Supplementary Appendix 2**.

Results
STUDY SUBJECTS
A total of 191 patients were included in the trial and randomly assigned to undergo treatment with BVS (95 patients) or CoCr-EES (96 patients). Six-month follow-up OCT data were available in 84 lesions in the BVS arm vs. 87 lesions in the CoCr-EES arm.

Baseline demographics and procedural characteristics have been reported previously and are presented in **Supplementary Table 1**[11]. Medication at discharge and six-month follow-up is summarised in **Supplementary Table 2**. No differences were observed in the antiplatelet regimens and statin use between the two arms.

OFDI ANALYSIS
Table 1 summarises the OFDI results of the neointimal assessments. The entire neointima area was comparable between the two arms. Superficial neointima and deep neointima were also similar between the two arms. The mean strut area of BVS was significantly larger than that of CoCr-EES.

The light property analysis **(Table 1, Figure 3, Figure 4)** was feasible in 82 lesions in the BVS arm vs. 87 lesions in the CoCr-EES arm, except for two lesions with incompatible data format. To facilitate the understanding of the three-parameter distribution (light attenuation, backscatter, and light intensity) in BVS and CoCr-EES, three-dimensional scatter plots were created **(Figure 4)**. In the entire lesion-level analysis **(Table 1)**, superficial, deep and entire neointima on BVS struts presented lower light attenuation than on CoCr-EES. Superficial neointima on BVS struts showed comparable backscatter as compared to that of CoCr-EES, while deep neointima of BVS showed lower backscatter than that of CoCr-EES. Light intensity of superficial neointima was comparable between the two arms, whereas light intensity of deep neointima was lower in the BVS arm than in the CoCr-EES arm. The SD of light attenuation and backscatter was higher in the CoCr-EES arm than in the BVS arm, while the SD of light intensity was comparable between the two arms.
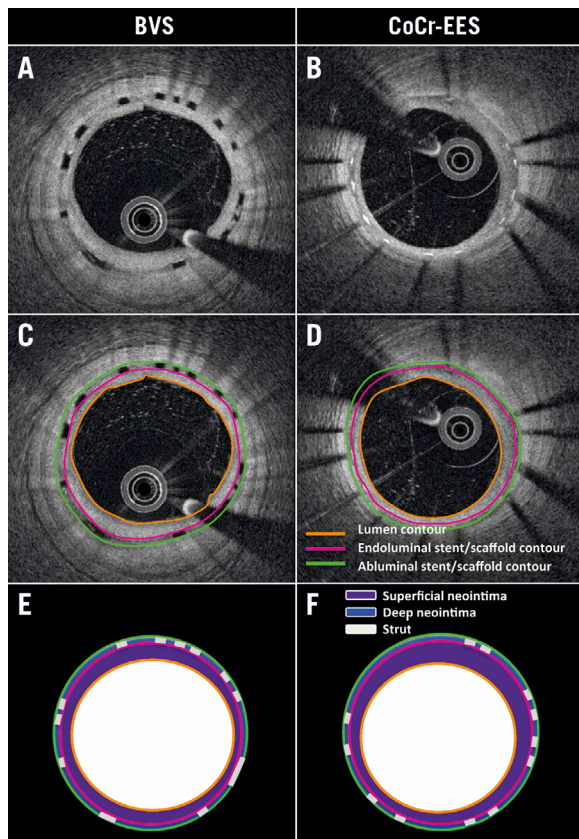
Figure 2. *Neointimal area compartments analysed by optical coherence tomography. Raw image examples of OFDI at six-month follow-up for BVS (A) and CoCr-EES (B). Lumen contour (orange), endoluminal (pink) and abluminal (green) stent/scaffold contours were delineated semi-automatically by the core lab (C, D). Light property analysis was separately computed for the following areas: 1) superficial neointima (purple area in E & F); 2) deep neointima (blue area in E & F); 3) entire neointima (purple and blue area in E & F).*

Table 1. Six-month quantitative neointimal assessments on OFDI.

	BVS N=84	CoCr-EES N=87	Difference [95% CI]	*p*-value
Mean neointimal area (superficial), mm²	0.65±0.27	0.64±0.46	0.01 [−0.10, 0.13]	0.838
Mean neointimal area (deep), mm²	0.61±0.15	0.64±0.12	−0.02 [−0.06, 0.02]	0.328
Mean neointimal area (entire), mm²	1.26±0.38	1.27±0.54	−0.01 [−0.15, 0.13]	0.909
Mean strut area, mm²	0.26±0.04	0.08±0.01	0.18 [0.17, 0.19]	<0.001
Mean neointimal thickness, mm	0.11±0.03	0.09±0.05	0.02 [0.01, 0.03]	<0.001
Maximal neointimal thickness, mm	0.32±0.12	0.34±0.19	−0.01 [−0.06, 0.03]	0.56
Light property analysis	**N=82**	**N=87**		
Superficial neointima				
Light attenuation (mean), mm⁻¹	0.77±0.15	1.27±0.55	−0.50 [−0.63, −0.38]	<0.001
Light attenuation (SD), mm⁻¹	0.63±0.11	1.64±0.76	−1.01 [−1.18, −0.84]	<0.001
Backscatter (mean)	4.81±0.52	4.94±0.61	−0.13 [−0.30, 0.04]	0.141
Backscatter (SD)	1.06±0.11	1.15±0.13	−0.09 [−0.12, −0.05]	<0.001
Light intensity (mean)	139±13	144±30	−4 [−11, 3]	0.236
Light intensity (SD)	34±3	43±53	−9 [−21, 2]	0.112
Deep neointima				
Light attenuation (mean), mm⁻¹	0.88±0.20	1.17±0.27	−0.29 [−0.37, −0.22]	<0.001
Light attenuation (SD), mm⁻¹	0.79±0.14	1.14±0.23	−0.35 [−0.41, −0.29]	<0.001
Backscatter (mean)	4.60±0.62	4.97±0.62	−0.37 [−0.56, −0.18]	<0.001
Backscatter (SD)	1.43±0.19	1.35±0.22	0.09 [0.02, 0.15]	0.006
Light intensity (mean)	129±14	138±21	−10 [−15, −4]	<0.001
Light intensity (SD)	41±4	44±26	−3 [−8, 3]	0.366
Entire neointima (superficial and deep)				
Light attenuation (mean), mm⁻¹	0.91±0.17	1.24±0.28	−0.34 [−0.41, −0.26]	<0.001
Light attenuation (SD), mm⁻¹	0.76±0.13	1.40±0.31	−0.64 [−0.72, −0.57]	<0.001
Backscatter (mean)	4.97±0.50	5.15±0.52	−0.18 [−0.34, −0.03]	0.021
Backscatter (SD)	1.12±0.11	1.17±0.13	−0.05 [−0.09, −0.01]	0.009
Light intensity (mean)	140±12	146±24	−6 [−12, 0]	0.053
Light intensity (SD)	36±3	42±37	−7 [−15, 2]	0.112

Data are expressed as mean±standard deviation (SD). CI: confidence interval

Discussion

The major findings of the present study can be summarised as follows: 1) in STEMI patients at six-month follow-up, superficial and deep neointima on BVS presented a lower light attenuation than that of CoCr-EES; 2) superficial neointima on BVS showed comparable backscatter to that of CoCr-EES, while deep neointima in BVS showed lower backscatter than that of CoCr-EES; 3) light intensity of superficial neointima was comparable between the two arms, whereas light intensity of deep neointima was lower in the BVS arm than in the CoCr-EES arm; and 4) the SD of light attenuation and backscatter was higher in the CoCr-EES arm than in the BVS arm.

HEAD-TO-HEAD COMPARISON OF NEOINTIMAL QUALITY IN PREVIOUS PUBLICATIONS

In the metallic stent era, a greater incidence of lipid-rich plaque was found in the drug-eluting stent than in the bare metal stent in the early phase (<9 months after device implantation)[16]. After the advent of the bioresorbable scaffold, OCT comparison of neointimal quality following implantation of BVS and CoCr-EES was performed in a *post hoc* analysis of the pooled data from the RESOLUTE and ABSORB cohort B trials[17]. In that stable angina cohort, visual quality assessment of neointima after implantation of BVS and CoCr-EES demonstrated that there was a trend towards a higher heterogenic tissue pattern of neointima (21.1% vs. 6.5%; p=0.12) with CoCr-EES than with BVS[17]. However, the comparison of neointimal quality following polymeric scaffold and metallic stent implantation has never been examined in the context of a randomised trial in a STEMI population. The current study evaluated the neointimal quality in a quantitative and highly objective way and demonstrated a higher SD of light attenuation and backscatter of neointima following CoCr-EES implantation than following BVS implantation, which could represent a higher heterogeneity of the neointimal quality in the CoCr-EES arm. Although the current cohort was a STEMI population, which was different from the previously studied stable angina population, similar observations were
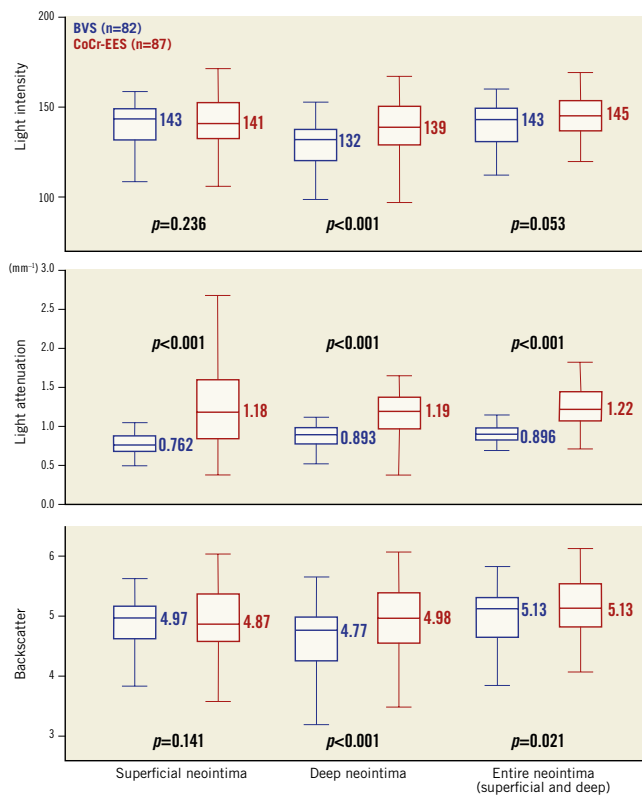
Figure 3. *Neointimal quality assessment by light property analysis. Neointimal quality was quantitatively assessed for BVS (blue) and CoCr-EES (red) by light property analysis including light intensity (upper panel), light attenuation (middle panel) and backscatter (lower panel). Neointimal area was separated into three parts: 1) superficial neointima, 2) deep neointima, and 3) entire neointima (superficial and deep).*

Figure 4. *Three-dimensional plots of light intensity, light attenuation and backscatter. Light intensity, light attenuation and backscatter results for superficial neointima (A), deep neointima (B), and entire neointima (superficial and deep) (C) illustrated in three-dimensional scatter plots for BVS (blue plot) and CoCr-EES (red plot).*

made. Furthermore, these observations are presented in a more comprehensive, quantitative and more objective manner than the visual (qualitative) assessment used in the previous study.

INTERPRETATION OF THE LIGHT PROPERTIES

As previously reported, lipid-rich plaque, necrotic core and macrophage infiltration exhibit strong light attenuation and backscatter, while calcific and fibrous tissue have a lower light attenuation and backscatter[5-7]. Our group also validated our software with histology and demonstrated the similar relationship with tissue characteristics[15]. Light intensity is correlated with maturation of the neointimal tissue[9]. In animal and human autopsy specimens, mature neointimal tissue with a predominance of smooth muscle cells consistently showed higher greyscale signal intensity values, whereas immature tissue with fibre-rich extracellular matrix, infrequent smooth muscle cells, interspersed inflammatory cells, macrophages and fibrin showed lower signal intensity values.

The present study shows comparable light intensity and higher light attenuation/backscatter of the superficial neointima of the CoCr-EES struts than that of the BVS struts. This could suggest that the presence of lipid components in the neointima (lipid
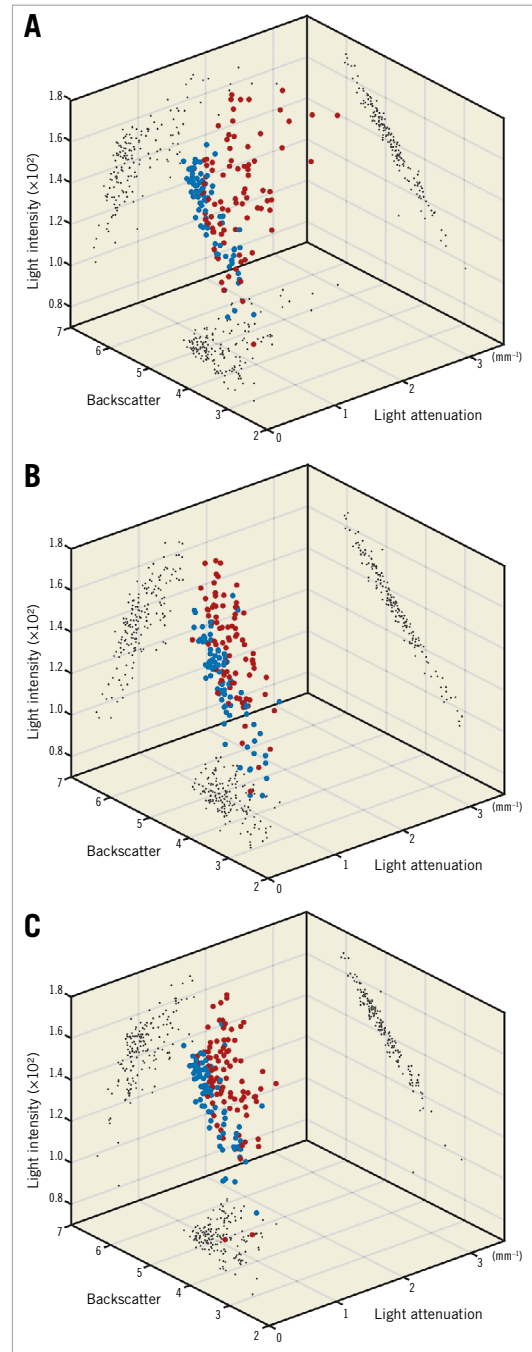
plaque and foam cell) might be more prominent after CoCr-EES than following BVS implantation in the early phase (six months). In other words, superficial neointima was more stable on the BVS than on the CoCr-EES. On the other hand, deep neointima in BVS struts showed low light attenuation, low backscatter and low light intensity, which would be compatible with the feature of PSLIA. The PSLIA was considered as a representation of vascular oedema,

fibrin deposition, plaque vulnerability, peri-strut inflammation, and immature tissue[9,18]. Although the incidence of PSLIA did not differ between the two arms (98.8% [81/82] vs. 98.9% [86/87] in BVS vs. CoCr-EES, respectively [p=0.966]), the current quantitative results of the light property analysis suggest a more prominent inflammation, more frequent fibre-rich extracellular matrix (proteoglycan which is known to be thrombogenic) with infrequent smooth muscle cells and more prominent fibrin deposition (the remnant of thrombus) in the vicinity of BVS struts compared to CoCr-EES struts[19]. It still remains unknown whether the PSLIA is implicated in scaffold thrombosis or is just a bystander. The present study, however, indicated that the PSLIA was encapsulated by the superficial stable neointima (dubbed "neo media") on top of the BVS[20]. When encapsulated, the high-risk deep neointima would not come into direct contact with blood and thus theoretically would not cause scaffold thrombosis at the time of a disruptive dismantling of the strut (late strut discontinuity[21]) **(Figure 5)**.

Of note, since the current population comprised STEMI patients, protruding necrotic core compartment and/or organised thrombus need to be taken into consideration as a neointimal component. Although the vessel condition (necrotic core and thrombus) should be the same in both the BVS and CoCr-EES arms, footprint differences (BVS 27% vs. CoCr-EES 13%) could result in a different amount of tissue protrusion[22]. In addition, the image characteristics of organised thrombus are not well understood or validated. Therefore, the abovementioned interpretation should be considered with caution. Further prospective serial imaging assessments with a histological approach and well-validated OCT methodology would be warranted to address the issue.

CLINICAL IMPLICATIONS

The present study demonstrated the dissimilar property of neointima following the implantation of BVS and CoCr-EES. Nonetheless, the direct impact of these findings on clinical outcome still remains to be elucidated. Recent randomised trials comparing BVS vs. CoCr-EES in patients with stable coronary disease (ABSORB II and ABSORB Japan trials) demonstrated increased late clinical events (very late scaffold thrombosis) in the BVS arm, although the observation did not reach a statistical significance to detect a difference between the two devices. On the other hand, two-year follow-up data in the current STEMI population cohort demonstrated comparable late events (one case of very late scaffold/stent thrombosis in each arm).

Both the primary endpoint of the TROFI II trial (healing score) and the current results of light property analysis suggest more stable and less lipid neointima formation after BVS implantation, which appears to be supportive for BVS usage in a STEMI population. However, future trials powered for clinical endpoints are needed to assess the risks and benefits of BVS use in STEMI patients.

Strengths and limitations

The current study compared the neointimal quality after the implantation of BVS and CoCr-EES in a randomised trial using dedicated fully automatic software. The novel neointimal assessment was quantitative and highly reproducible. Other possible confounding factors such as smoking and statin usage should be cancelled out by randomisation. However, some limitations need to be acknowledged. First, the study population included only STEMI patients. Caution should therefore be employed in extrapolating the present observations beyond the specific subset of STEMI patients, whose lesions and biologic responses may or may not be applicable to non-STEMI or stable coronary lesions. Second, the follow-up time of the present study was six months. Maturation of neointimal coverage might still be ongoing. Taniguchi et al reported that the incidence of PSLIA of the CoCr-EES decreased from one- to two-year follow-up[23]. Third, since baseline OCT images were not available in the TROFI II trial, plaque morphology pre stent/scaffold implantation could not be assessed. Fourth, procedural differences between the two arms **(Supplementary Table 1)** could have
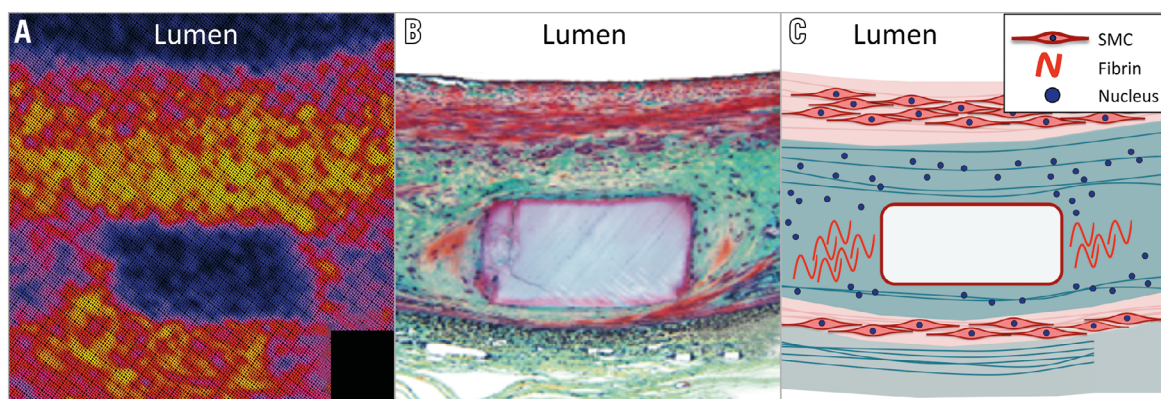
Figure 5. *Encapsulation of the underlying thrombogenic neointima. A) Strut core image with peri-strut low-intensity area on optical coherence tomography (light intensity analysis). B) Histological image stained by Movat's pentachrome staining (red: smooth muscle cell/protein; blue-green: provisional matrix with staining characteristics comparable to that of proteoglycan; yellow: collagen). C) The tissue on top of the struts creates a homogeneous endoluminal tissue layer, consisting mainly of smooth muscle cells (dubbed "neo media")[20]. This tissue layer encapsulates the underlying thrombogenic tissue. SMC: smooth muscle cells*

partially impacted on the current results. Lastly, the light property can be affected by the residual blood or intraluminal mass. Although the core laboratory confirmed the sufficient quality of the OFDI images, it could confound the current results. Further serial assessments at long-term follow-up would be warranted.

Conclusions

OFDI comparison in STEMI patients at six-month follow-up demonstrated the comparable light intensity and lower light attenuation/ backscatter of the superficial neointima after BVS implantation than after CoCr-EES implantation, suggesting that tissue maturation was comparable but the lipidic change of neointima was less prominent after BVS implantation. The clinical implications of the differential neointimal properties still remain to be investigated in future trials. A trial with clinically oriented endpoints would be warranted to investigate the risks and benefits of BVS in a STEMI population.

Impact on daily practice

The present study demonstrated the dissimilar property of neointima following the implantation of BVS and CoCr-EES. Both the primary endpoint of the TROFI II trial (healing score) and the current results of light property analysis suggest more stable and less lipid neointima formation after BVS implantation, which appears to be supportive for BVS usage in a STEMI population. However, future trials powered for clinical endpoints are needed to assess the risks and benefits of BVS use in STEMI patients.

Guest Editor

This paper was guest edited by Alec Vahanian, MD, PhD; Department of Cardiology, Hôpital Bichat, Paris and University Paris VII, Paris, France.

Conflict of interest statement

Y. Sotomi has received speaker honoraria from Abbott Vascular Japan and research grants from the Fukuda Memorial Foundation for Medical Research and SUNRISE lab. Y. Onuma is a member of the Advisory Board for Abbott Vascular and has received speaker honoraria from Terumo. L. Räber has received speaker fees and research grants to the institution from St. Jude Medical. M. Sabaté is a consultant for Abbott Vascular. P.W. Serruys is a member of the Advisory Board for Abbott Vascular. The other authors have no conflicts of interest to declare. The Guest Editor is a consultant for Edwards Lifesciences.

References

1. Onuma Y, Sotomi Y, Shiomi H, Ozaki Y, Namiki A, Yasuda S, Ueno T, Ando K, Furuya J, Igarashi K, Kozuma K, Tanabe K, Kusano H, Rapoza R, Popma JJ, Stone GW, Simonton C, Serruys PW, Kimura T. Two-year clinical, angiographic, and serial optical coherence tomographic follow-up after implantation of an everolimus-eluting bioresorbable scaffold and an everolimus-eluting metallic stent: insights from the randomised ABSORB Japan trial. *EuroIntervention.* 2016;12:1090-101.

2. Serruys PW, Chevalier B, Sotomi Y, Cequier A, Carrié D, Piek JJ, Van Boven AJ, Dominici M, Dudek D, McClean D, Helqvist S, Haude M, Reith S, de Sousa Almeida M, Campo G, Iniguez A, Sabaté M, Windecker S, Onuma Y. Comparison of an everolimus-eluting bioresorbable scaffold with an everolimus-eluting metallic stent for the treatment of coronary artery stenosis (ABSORB II): a 3 year, randomised, controlled, single-blind, multicentre clinical trial. *Lancet.* 2016;388:2479-91.

3. Sotomi Y, Suwannasom P, Serruys PW, Onuma Y. Possible mechanical causes of scaffold thrombosis: insights from case reports with intracoronary imaging. *EuroIntervention.* 2017;12:1747-56.

4. Otake H, Shite J, Ikeno F, Shinke T, Teramoto T, Miyoshi N, Ako J, Honda Y, Fitzgerald PJ, Hirata K. Evaluation of the peri-strut low intensity area following sirolimus- and paclitaxel-eluting stents implantation: insights from an optical coherence tomography study in humans. *Int J Cardiol.* 2012;157:38-42.

5. Xu C, Schmitt JM, Carlier SG, Virmani R. Characterization of atherosclerosis plaques by measuring both backscattering and attenuation coefficients in optical coherence tomography. *J Biomed Opt.* 2008;13:034003.

6. Imanaka T, Fujii K, Hao H, Shibuya M, Saita T, Kawakami R, Fukunaga M, Kawai K, Tamaru H, Miki K, Horimatsu T, Sumiyoshi A, Nishimura M, Hirota S, Masuyama T, Ishihara M. Ex vivo assessment of neointimal characteristics after drug-eluting stent implantation: Optical coherence tomography and histopathology validation study. *Int J Cardiol.* 2016;221:1043-7.

7. van Soest G, Goderie T, Regar E, Koljenovic S, van Leenders GL, Gonzalo N, van Noorden S, Okamura T, Bouma BE, Tearney GJ, Oosterhuis JW, Serruys PW, van der Steen AF. Atherosclerotic tissue characterization in vivo by optical coherence tomography attenuation imaging. *J Biomed Opt.* 2010;15:011105.

8. Nakano M, Vorpahl M, Otsuka F, Taniwaki M, Yazdani SK, Finn AV, Ladich ER, Kolodgie FD, Virmani R. Ex vivo assessment of vascular response to coronary stents by optical frequency domain imaging. *JACC Cardiovasc Imaging.* 2012;5:71-82.

9. Malle C, Tada T, Steigerwald K, Ughi GJ, Schuster T, Nakano M, Massberg S, Jehle J, Guagliumi G, Kastrati A, Virmani R, Byrne RA, Joner M. Tissue characterization after drug-eluting stent implantation using optical coherence tomography. *Arterioscler Thromb Vasc Biol.* 2013;33:1376-83.

10. Nakatani S, Ishibashi Y, Sotomi Y, Perkins L, Eggermont J, Grundeken MJ, Dijkstra J, Rapoza R, Virmani R, Serruys PW, Onuma Y. Bioresorption and Vessel Wall Integration of a Fully Bioresorbable Polymeric Everolimus-Eluting Scaffold: Optical Coherence Tomography, Intravascular Ultrasound, and Histological Study in a Porcine Model With 4-Year Follow-Up. *JACC Cardiovasc Interv.* 2016;9:838-51.

11. Sabaté M, Windecker S, Iniguez A, Okkels-Jensen L, Cequier A, Brugaletta S, Hofma SH, Räber L, Christiansen EH, Suttorp M, Pilgrim T, Anne van Es G, Sotomi Y, Garcia-Garcia HM, Onuma Y, Serruys PW. Everolimus-eluting bioresorbable stent vs. durable polymer everolimus-eluting metallic stent in patients with ST-segment elevation myocardial infarction: results of the randomized ABSORB ST-segment elevation myocardial infarction-TROFI II trial. *Eur Heart J.* 2016;37:229-40.

12. Authors/Task Force members, Windecker S, Kolh P, Alfonso F, Collet JP, Cremer J, Falk V, Filippatos G, Hamm C, Head SJ, Jüni P, Kappetein AP, Kastrati A, Knuuti J, Landmesser U, Laufer G, Neumann FJ, Richter DJ, Schauerte P, Sousa Uva M, Stefanini GG, Taggart DP, Torracca L, Valgimigli M, Wijns W, Witkowski A. 2014 ESC/EACTS Guidelines on myocardial revascularization: The Task Force on Myocardial Revascularization of the European Society of Cardiology (ESC) and the European Association for Cardio-Thoracic Surgery (EACTS)Developed with the special contribution of the European Association of Percutaneous Cardiovascular Interventions (EAPCI). *Eur Heart J.* 2014;35:2541-619.

13. Räber L, Onuma Y, Brugaletta S, Garcia-Garcia HM, Backx B, Iniguez A, Okkels Jensen L, Cequier-Fillat A, Pilgrim T, Christiansen EH, Hofma SH, Suttorp M, Serruys PW, Sabate M, Windecker S. Arterial healing following primary PCI using the Absorb everolimus-eluting bioresorbable vascular scaffold (Absorb BVS) versus the durable polymer everolimus-eluting metallic stent (XIENCE) in patients with acute ST-elevation myocardial infarction: rationale and design of the randomised TROFI II study. *EuroIntervention.* 2016;12:482-9.

14. Nakatani S, Sotomi Y, Ishibashi Y, Grundeken MJ, Tateishi H, Tenekecioglu E, Zeng Y, Suwannasom P, Regar E, Radu MD, Räber L, Bezerra H, Costa MA, Fitzgerald P, Prati F, Costa RA, Dijkstra J, Kimura T, Kozuma K, Tanabe K, Akasaka T, Di Mario C, Serruys PW, Onuma Y. Comparative analysis method of permanent metallic stents (XIENCE) and bioresorbable poly-L-lactic (PLLA) scaffolds (Absorb) on optical coherence tomography at baseline and follow-up. *EuroIntervention.* 2016;12:1498-509.

15. Liu S, Sotomi Y, Eggermont J, Nakazawa G, Torii S, Ijichi T, Onuma Y, Serruys PW, Lelieveldt BPF, Dijkstra J. Tissue characterization with depth-resolved attenuation coefficient and backscatter term in intravascular optical coherence tomography images. *J Biomed Opt.* 2017;22:1-16.

16. Yonetsu T, Kim JS, Kato K, Kim SJ, Xing L, Yeh RW, Sakhuja R, McNulty I, Lee H, Zhang S, Uemura S, Yu B, Kakuta T, Jang IK. Comparison of incidence and time course of neoatherosclerosis between bare metal stents and drug-eluting stents using optical coherence tomography. *Am J Cardiol.* 2012;110:933-9.

17. Gomez-Lara J, Brugaletta S, Farooq V, Onuma Y, Diletti R, Windecker S, Thuesen L, McClean D, Koolen J, Whitbourn R, Dudek D, Smits PC, Chevalier B, Regar E, Veldhof S, Rapoza R, Ormiston JA, Garcia-Garcia HM, Serruys PW. Head-to-head comparison of the neointimal response between metallic and bioresorbable everolimus-eluting scaffolds using optical coherence tomography. *JACC Cardiovasc Interv.* 2011;4:1271-80.

18. Tellez A, Afari ME, Buszman PP, Seifert P, Cheng Y, Milewski K, McGregor JC, Garza JA, Roberts MB, Yi GH, Kaluza GL, Granada JF. Peri-strut low-intensity areas in optical coherence tomography correlate with peri-strut inflammation and neointimal proliferation: an in-vivo correlation study in the familial hypercholesterolemic coronary swine model of in-stent restenosis. *Coron Artery Dis.* 2014;25:595-601.

19. Otsuka F, Pacheco E, Perkins LE, Lane JP, Wang Q, Kamberi M, Frie M, Wang J, Sakakura K, Yahagi K, Ladich E, Rapoza RJ, Kolodgie FD, Virmani R. Long-term safety of an everolimus-eluting bioresorbable vascular scaffold and the cobalt-chromium XIENCE V stent in a porcine coronary artery model. *Circ Cardiovasc Interv.* 2014;7:330-42.

20. Serruys PW, Ormiston J, van Geuns RJ, de Bruyne B, Dudek D, Christiansen E, Chevalier B, Smits P, McClean D, Koolen J, Windecker S, Whitbourn R, Meredith I, Wasungu L, Ediebah D, Veldhof S, Onuma Y. A Polylactide Bioresorbable Scaffold Eluting Everolimus for Treatment of Coronary Stenosis: 5-Year Follow-Up. *J Am Coll Cardiol.* 2016;67:766-76.

21. Onuma Y, Serruys PW, Muramatsu T, Nakatani S, van Geuns RJ, de Bruyne B, Dudek D, Christiansen E, Smits PC, Chevalier B, McClean D, Koolen J, Windecker S, Whitbourn R, Meredith I, Garcia-Garcia HM, Veldhof S, Rapoza R, Ormiston JA. Incidence and imaging outcomes of acute scaffold disruption and late structural discontinuity after implantation of the absorb Everolimus-Eluting fully bioresorbable vascular scaffold: optical coherence tomography assessment in the ABSORB cohort B Trial (A Clinical Evaluation of the Bioabsorbable Everolimus Eluting Coronary Stent System in the Treatment of Patients With De Novo Native Coronary Artery Lesions). *JACC Cardiovasc Interv.* 2014;7:1400-11.

22. Sotomi Y, Suwannasom P, Tenekecioglu E, Tateishi H, Abdelghani M, Serruys PW, Onuma Y. Differential aspects between cobalt-chromium everolimus drug-eluting stent and Absorb everolimus bioresorbable vascular scaffold: from bench to clinical use. *Expert Rev Cardiovasc Ther.* 2015;13:1127-45.

23. Taniguchi Y, Otake H, Shinke T, Nakagawa M, Hariki H, Inoue T, Osue T, Hiranuma N, Nishio R, Kinutani H, Iwasaki M, Konishi A, Kuroda M, Hirata K. Two-year vessel healing after everolimus-eluting stent implantation: serial assessment by optical coherence tomography. *J Cardiol.* 2015;65:298-304.

Supplementary data

Supplementary Appendix 1. PCI procedure.
Supplementary Appendix 2. Statistical analysis.
Supplementary Table 1. Patient demographics and procedural characteristics.
Supplementary Table 2. Medication at discharge and 6-month follow-up.

The supplementary data are published online at:
http://www.pcronline.com/
eurointervention/139th_issue/117

Supplementary data

Supplementary Appendix 1. PCI procedure

Primary percutaneous coronary intervention (PCI) was performed according to standard practice.[11, 12] As per protocol, manual thrombectomy was mandatory to reduce thrombus burden. The decision to perform pre- or post-dilatation was left to the operator's discretion. If these techniques were performed, specific rules had to be followed during the procedure as well as for scaffold/stent sizing.[13] Scaffold implantation was carried out following current standards.[13] The other details were previously reported elsewhere.[11] It was recommended that patients receive a loading dose of aspirin and a $P2Y_{12}$ inhibitor pre-procedure, followed by dual antiplatelet therapy for at least 12 months. Optimal medical therapy was mandated in all patients.[12]

Supplementary Appendix 2. Statistical analysis

Data are expressed as mean ± SD or median and interquartile range with differences [95% confidence interval]. Group means for continuous variables with normal and non-normal distributions were compared using Student's t-tests and Mann-Whitney U tests, respectively. Categorical variables were compared using the Pearson's chi-square test or Fisher's exact test, as appropriate. Mixed linear model with an assumed Gaussian distribution was used for the comparisons of continuous variables to take into account the clustered nature of >1 scaffolds analysed from the same patients, which might result in unknown correlations among measurements within the clusters. Statistical significance was assumed at a probability (p) value of <0.05. All statistical analyses were performed with SPSS, Version 24.0.0 (IBM Corp., Armonk, NY, USA).

Supplementary Table 1. Patient demographics and procedural characteristics.

	BVS	CoCr-EES	Difference [95% confidence interval]
Patient	**N=95**	**N=96**	
Male, n (%)	73 (76.8)	84 (87.5)	-10.7% [-21.4%, 0.1%]
Age, years	59.1±10.7	58.2±9.6	0.9 [-2.0, 3.8]
Current smoking, n (%)	46 (48.4)	47 (49.5)	-1.1% [-15.3%, 13.2%]
Previous smoking, n (%)	22 (23.2)	22 (23.2)	0.0% [-12.0%, 12.0%]
Diabetes mellitus, n (%)	18 (18.9)	14 (14.7)	4.2% [-6.4%, 14.8%]
Insulin-dependent, n (%)	5 (5.3)	3 (3.2)	2.1% [-3.6%, 7.8%]
Non-insulin-dependent, n (%)	13 (13.7)	11 (11.6)	2.1% [-7.3%, 11.5%]
Hypertension, n (%)	41 (44.1)	35 (36.5)	7.6% [-6.3%, 21.6%]
Hypercholesterolemia, n (%)	60 (63.8)	55 (57.3)	6.5% [-7.3%, 20.4%]
LDL cholesterol (mmol/L)*	3.1±0.8	3.1±1.2	-0.0 [-0.4, 0.3]
Chronic obstructive pulmonary disease, n (%)	3 (3.2)	3 (3.1)	0.0% [-4.9%, 5.0%]
Body mass index, kg/m^2	27.0±4.1	27.7±4.2	-0.7 [-1.9, 0.5]
Lesions	**N=95**	**N=98**	
Infarct-related target lesions			
Right coronary artery, n (%)	44 (46.3)	44 (44.9)	1.4% [-12.6%, 15.5%]
Left anterior descending artery, n (%)	34 (35.8)	41 (41.8)	-6.0% [-19.8%, 7.7%]
Left circumflex artery, n (%)	17 (17.9)	13 (13.3)	4.6% [-5.6%, 14.9%]
Successful thrombectomy, n (%)	89 (81.1)	72 (73.5)	7.6 [-4.2, 19.4]
Mode of stenting			
Direct stenting, n (%)	42 (44.2)	48 (49.0)	-4.8 [-18.8, 9.3]
Predilatation, n (%)	53 (55.8)	50 (51.0)	4.8 [-9.3, 18.8]
Grade of perfusion			
TIMI 0, n (%)	60 (63.2)	61 (62.9)	0.3% [-13.4%, 13.9%]
TIMI 1. n (%)	3 (3.2)	3 (3.1)	0.1% [-4.9%, 5.0%]
TIMI 2, n (%)	8 (8.4)	13 (13.4)	-5.0% [-13.8%, 3.8%]
TIMI 3, n (%)	24 (25.3)	20 (20.6)	4.6% [-7.2%, 16.5%]
Device deployment			

Number of study devices	1.2±0.4	1.1±0.4	0.0 [-0.1, 0.2]
Nominal length of scaffold/stent	20.6±5.8	20.7±6.7	-0.1 [-1.8, 1.5]
Nominal diameter of scaffold/stent	3.25±0.30	3.12±0.37	0.13 [0.04, 0.22]
Maximum deployment pressure, atm	14.1±3.8	13.3±3.0	0.8 [-0.6, 2.1]
Post-dilatation performed, n (%)	48 (50.5)	25 (25.5)	25.0 [11.8, 38.3]
Use of non-compliant balloon, n (%)	43 (89.6)	13 (52.0)	37.6 [16.2, 59.0]
Diameter of post-dilatation balloon, mm	3.51±0.34	3.29±0.62	0.22 [-0.01, 0.44]
Maximum pressure, atm	15.8±3.4	18.6±3.9	-2.9 [-4.6, -1.1]
Device success, n (%)	91 (95.8)	98 (100.0)	-4.2 [-8.2, -0.2]
Procedure success, n (%)	91 (95.8)	96 (100.0)	-4.2 [-8.2, -0.2]

Data are expressed as number (%) or mean ± standard deviation. N refers to number of patients or lesions with data available. *BVS: N=69 vs. CoCr-EES: N=64.

Supplementary Table 2. Medication at discharge and 6-month follow-up.

	BVS N=95	CoCr-EES N=96	Difference [95% confidence interval]	*p*-value
Medication at discharge				
Acetylsalicylic acid	100.0% (95/95)	99.0% (95/96)	1.0% [-1.0%, 3.1%]	1
Acetylsalicylic acid + Ticagrelor	54.7% (52/95)	55.2% (53/96)	-0.5% [-14.6%, 13.6%]	0.95
Acetylsalicylic acid + Prasugrel	30.5% (29/95)	40.0% (38/95)	-9.5% [-23.0%, 4.0%]	0.17
Other antiplatelet	10.9% (10/92)	3.2% (3/94)	7.7% [0.4%, 15.0%]	0.04
ACE inhibitor	57.9% (55/95)	56.8% (54/95)	1.1% [-13.0%, 15.1%]	0.88
Oral anticoagulation	0.0% (0/95)	2.1% (2/95)	-2.1% [-5.0%, 0.8%]	0.5
AT-II	5.3% (5/95)	10.5% (10/95)	-5.3% [-12.9%, 2.4%]	0.18
Beta-blocker	78.9% (75/95)	74.5% (70/94)	4.5% [-7.6%, 16.5%]	0.47
Statins	94.7% (90/95)	94.7% (90/95)	0.0% [-6.4%, 6.4%]	1
Atorvastatin	73.7% (70/95)	73.7% (70/95)	0.0% [-12.5%, 12.5%]	1
Rosuvastatin	11.6% (11/95)	10.5% (10/95)	1.1% [-7.9%, 10.0%]	0.82
Others	9.5% (9/95)	10.5% (10/95)	-1.1% [-9.6%, 7.5%]	0.81
Other lipid-lowering drugs	6.3% (6/95)	2.1% (2/95)	4.2% [-1.5%, 9.9%]	0.28
Gastric protection drug	60.0% (57/95)	68.4% (65/95)	-8.4% [-22.0%, 5.2%]	0.23
Medication at 6 months				
Acetylsalicylic acid	98.9% (90/91)	96.9% (93/96)	2.0% [-2.1%, 6.1%]	0.62
Acetylsalicylic acid + Ticagrelor	47.3% (43/91)	49.0% (47/96)	-1.7% [-16.0%, 12.6%]	0.82
Acetylsalicylic acid + Prasugrel	31.9% (29/91)	37.9% (36/95)	-6.0% [-19.7%, 7.6%]	0.39
Other antiplatelet	2.2% (2/90)	5.2% (5/96)	-3.0% [-8.4%, 2.4%]	0.45
ACE inhibitor	54.9% (50/91)	53.7% (51/95)	1.3% [-13.1%, 15.6%]	0.86
Oral anticoagulation	1.1% (1/91)	3.2% (3/95)	-2.1% [-6.2%, 2.1%]	0.62
AT-II	6.6% (6/91)	16.8% (16/95)	-10.2% [-19.3%, -1.2%]	0.03
Beta-blocker	86.8% (79/91)	82.1% (78/95)	4.7% [-5.7%, 15.1%]	0.38
Statins	95.6% (86/90)	92.6% (88/95)	2.9% [-3.8%, 9.7%]	0.4
Atorvastatin	77.8% (70/90)	73.7% (70/95)	4.1% [-8.2%, 16.4%]	0.52
Rosuvastatin	7.8% (7/90)	11.6% (11/95)	-3.8% [-12.3%, 4.7%]	0.38
Other	10.0% (9/90)	7.4% (7/95)	2.6% [-5.5%, 10.8%]	0.52

Other lipid-lowering drugs	7.7% (7/91)	0.0% (0/95)	7.7% [2.2%, 13.2%]	0.006
Gastric protection drug	59.3% (54/91)	58.9% (56/95)	0.4% [-13.7%, 14.5%]	0.96

Data are expressed as percentage (n/N). N refers to number of patients or lesions with data available.